Evaluation of hypoxic PET radiotracer in xenograft murine model after anti-angiogenesis treatment

Arthur Eung-Hyuck Cho

Department of Medicine

The Graduate School, Yonsei University

Evaluation of hypoxic PET radiotracer in xenograft murine model after anti-angiogenesis treatment

Directed by Professor Mijin Yun

The Doctoral Dissertation
submitted to the Department of Medicine
the Graduate School of Yonsei University
in partial fulfillment of the requirements for the degree
of Doctor of Philosophy

Arthur Eung-Hyuck Cho

December 2017

This certifies that the Doctoral Dissertation of Arthur Eung-Hyuck Cho is approved.

Thesis Supervisor : Mijin Yun

Thesis Committee Member#1 : Kyung Sik Kim

Thesis Committee Member#2 : Se Hoon Kim

Thesis Committee Member#3 : Byoung Chul Cho

Thesis Committee Member#4 : Tae Sung Kim

The Graduate School
Yonsei University

December 2017

ACKNOWLEDGEMENTS

I first thank God for providing me with the strength and inspiration in this research project.

Also, my deep gratitude for the understanding and support my wife Monica Jung and my family have given me during this period.

I thank my supervisor for her support, knowledge, and encouragement she has provided me on this project.

I would like to thank the Nuclear Medicine faculty, technicians, research assistants, radiopharmacologists for the countless hours of discussion and effort in helping me in the experiments. I would especially like to thank the radiopharmacologists Park Jun Young and Dr. Chun Joong-Hyun for their efforts in synthesizing the radiotracers despite their busy schedule.

<TABLE OF CONTENTS>

ABSTRACT ····· 1
I. INTRODUCTION ····· 5
II. MATERIALS AND METHODS ····· 8
1. In vitro studies ····· 8
2. In vivo studies ····· 11
A. Tumor model establishment and Avastin therapy ····· 11
B. Animal microPET and autoradiography protocol ····· 12
C. Histopathology and Imaging Analysis ····· 14
III. RESULTS ····· 16
1. In vitro studies ····· 16
2. In vivo studies ····· 18
A. Evaluation of Avastin therapy response in HCT116 cell lines ··· 18
B. Evaluation of ^{18}F-MISO retention in necrotic tumors ····· 20
3. In vitro studies in dependence of ^{18}F-MISO uptake according to pH and necrosis ····· 22
A. Dependence of ^{18}F-MISO uptake in pH and tumor acidity ····· 22
B. in vitro evaluation of ^{18}F-MISO uptake in necrotic cells ····· 23
4. In vitro and in vivo studies using ^{64}Cu-ATSM ····· 25
A. in vitro study ····· 25
B. in vivo study ····· 27
IV. DISCUSSION ····· 28
V. CONCLUSION ····· 33
REFERENCES ····· 34
ABSTRACT(IN KOREAN) ····· 39

LIST OF FIGURES

Figure 1. Timeline of Avastin therapy for hypoxic radiotracer assessment ····· 12
Figure 2. In vitro study on selection of tumor cell lines ····· 17
Figure 3. Tumor growth delay curve ····· 19
Figure 4. MicroPET scan showing uptake patterns in HCT116 tumors after Avastin therapy ····· 21
Figure 5. ^{18}F-MISO and ^{18}F-FDG autoradiography ····· 22
Figure 6. ^{18}F-MISO uptake dependence on extracellular pH · 23
Figure 7. Comparison of ^{18}F-MISO retention in necrotic conditions compared to hypoxic/normoxic HCT116 cells ·· 24
Figure 8. Correlation between ^{64}Cu-ATSM uptake before and after siRNA inhibition of HIF1a in (1%) hypoxic chamber · 26
Figure 9. ^{64}Cu-ATSM autoradiography of tumor with necrotic components ····· 27

LIST OF TABLES

Table 1. Comparison of immunohistologic changes after Avastin treatment in HCT 116 colon cancer cell line ····· 19
Table 2. Comparison of ^{18}F-FDG and ^{18}F-MISO uptake in control and treatment group ····· 20
Table 3. Comparison of hypoxic radiotracer retention in necrotic portions ····· 21

ABSTRACT

Evaluation of hypoxic PET radiotracer in xenograft murine model after anti-angiogenesis treatment

Arthur Eung-Hyuck Cho

Department of Medicine
The Graduate School, Yonsei University

(Directed by Professor Mijin Yun)

Purpose: Non-invasive assessment of tumor hypoxic extent is of clinical importance, as hypoxia is a known factor in chemotherapy or radiotherapy resistance. Anti-angiogenetic treatments have been developed to improve tumor hypoxia, but studies have shown that tumors may develop evasive resistance to anti-angiogenetic therapy. Non-invasive assessment of tumor hypoxia is needed to evaluate the temporal changes of hypoxia in tumors undergoing anti-angiogenesis therapy. Positron Emission Tomography (PET) radiotracers such as ^{18}F-misonidazole (^{18}F-MISO) and ^{64}Cu-diacetyl-di(N4-methylthiosemicarbazone) (^{64}Cu-ATSM) have been specifically developed to evaluate for hypoxic status of tumors, and ^{18}F-fluorodeoxyglucose (^{18}F-FDG) is also known to reflect hypoxic status of tumors. The purpose of this study is to evaluate the role of these PET radiotracers in evaluating angiogenesis response in xenograft murine model.

Materials and Methods: Human colorectal cancer cell line HCT116 was plated on 6 well plates and incubated in 1% O_2 hypoxic chamber or normoxic chamber (5% CO_2 in air) for 4 hours and 12 hours. ^{18}F-FDG, ^{18}F-MISO, and ^{64}Cu-ATSM were separately incubated, scraped, and counted for radioactivity. Western blot of HIF1a and GLUT1 of the cell lysates was performed to evaluate for cellular response to hypoxia induction. Finally, to evaluate for the effect of extracellular conditions on intracellular ^{18}F-MISO retention, ^{18}F-MISO evaluation was performed in cells incubated in acidic culture medium. Also, to evaluate for ^{18}F-MISO uptake in necrotic cells, cells were incubated in heat chamber (55^{o}C) to induce necrosis, as well as incubated in hypoxic chamber until necrosis was induced.

For in vivo studies on Avastin therapy response assessment, HCT116 was subcutaneously implanted into hind leg of BALB/c-nu mice. ^{18}F-FDG was obtained one day before therapy, and ^{18}F-MISO or ^{64}Cu-ATSM was obtained on the day of Avastin therapy. Immediately after hypoxic radiotracer PET scan, Avastin was injected intraperitoneally, 2 times a week for 2 weeks, during which tumor size changes were recorded. Both treatment and control mice had either a combination of ^{18}F-FDG/^{18}F-MISO or ^{18}F-FDG/^{64}Cu-ATSM post-therapy PET before sacrifice. Immediately after PET, the mice were sacrificed, tumors were excised, bisected, and half was put into formalin for pathologic evaluation, and half of tumor was frozen, cryosectioned, autoradiography images were acquired. The post-therapy PET radiotracer

administration was alternated so autoradiography images of all radiotracers were obtained for both control and treatment groups. Autoradiography images were reviewed to evaluate for radiotracer retention in necrotic areas. Immunohistochemical staining was performed to evaluate for pimonidazole (hypoxia), H&E, and Ki-67.

Results: In vitro studies showed higher hypoxic/normoxic cell retention ratio in ^{18}F-MISO or ^{64}Cu-ATSM radiotracers compared to ^{18}F-FDG. Western blot showed that HIF1a stabilization but minimal GLUT1 induction in hypoxic conditions. ^{18}F-MISO retention studies have shown a reduction of approximately 50% in acidic environment lower than pH of 6.9. Also, ^{18}F-MISO showed significantly higher retention in necrotic conditions compared to normoxic conditions, but not as high as hypoxic conditions.

In animal studies, Avastin treated group showed significant slower tumor growth compared to control group. Immunohistochemical analysis revealed significantly higher hypoxic areas in treatment group compared to control group (17.67% ± 5.95 vs 11.02 ±4.81, p=0.004). There was no significant difference in Ki-67 expression (41.69±22.58 vs 49.33±13.84, p=0.328) or % area of necrotic portions (36.02±24.8 vs 27.82±14.0, p=0.249). Post-therapy PET showed no significance difference in uptake between treatment or control groups (^{18}F-FDG: 5.4±6.4 vs 3.0±1.8, p=0.123; ^{18}F-MISO: 4.6±3.0 vs 4.6±2.7, p=0.953).

Autoradiography analysis of necrotic portions revealed significantly

higher ^{18}F-MISO (2.41±1.77) in necrotic portions of the tumor compared to ^{18}F-FDG (0.83±0.42, p=0.001) or ^{64}Cu-ATSM (0.94±0.48, p=0.005).

Conclusion: In subcutaneous tumor model for HCT116 colon cancer cell line, significant tumor growth suppression is seen after two weeks of Avastin therapy, as well as an increase in hypoxic portions. In tumors with necrotic portions, ^{64}Cu-ATSM PET may reflect non-viable portions better than ^{18}F-MISO PET.

Key words : Hypoxia, ^{18}F-FDG, ^{18}F-MISO, ^{64}Cu-ATSM, murine xenograft tumor, digital autoradiography, necrosis

Evaluation of hypoxic PET radiotracer in xenograft murine model after anti-angiogenesis treatment

Arthur Eung-Hyuck Cho

Department of Medicine
The Graduate School, Yonsei University

(Directed by Professor Mijin Yun)

I. INTRODUCTION

Angiogenesis is one of the hallmarks for tumors,[1] as proliferating tumors relies on angiogenesis to obtain oxygen and nutrients for growth. One of the cell signaling pathways that starts the cellular cascade to increased angiogenesis is hypoxia induced factor 1-alpha (HIF1a). In hypoxic conditions, stabilized HIF1a will start a signal cascade that will increase glycolysis, angiogenesis and changes in cell proliferation.[2,3] Therapeutic agents have been developed to target this reliance on angiogenesis. Recent studies have shown that these anti-angiogenesis agents in combination with chemotherapy or radiotherapy have significantly increased disease free survival.[4,5] However, other studies have shown that prolonged use of anti-angiogenesis treatment have paradoxically increased tumor hypoxia, which can lead to decreased efficacy of radiotherapy.[6-9] Further studies are needed to determine the optimal treatment

strategy for anti-angiogenesis agents.

Molecular imaging with Positron Emitting Tomography (PET) radiotracers has been increasingly been studied in evaluating therapy response. ^{18}F-misonidazole (^{18}F-MISO) has been extensively studied as a hypoxic tracer in the clinical and animal settings.[10-12] The current known mechanism of ^{18}F-MISO retention in hypoxic cells are the reduction of the NO2 group to NH2 via flavin-associated oxidoreductase enzymes. In the presence of oxygen, NO2 is reduced and re-oxidized in a futile loop by oxidoreductase enzymes, but when oxygen is less than <10 mmHg, these oxidoreductase enzymes reduce NO2 to NH2, after which NH2 reacts with macromolecular proteins, which results in ^{18}F-MISO being trapped within the hypoxic cells.[2] Also, due to the high lipophilicity of ^{18}F-MISO, delayed imaging is necessary during PET scans. However, one potential unevaluated factor that might also influence the biodistribution of ^{18}F-MISO in tumors may be the pH sensitive ring of the nitroimidazole ring.[13] ^{64}Cu-Diacetyl-bis(N(4)-methylthiosemicarbazone (^{64}Cu-ATSM) is another hypoxic tracer that has been evaluated in animal and clinical studies, but with different biodistribution and retention mechanisms than the nitroimidazole compounds.[14-16] Due to the lower lipophilicity of ^{64}Cu-ATSM, this radiotracer is more rapidly washed out of normal tissues, which allows better contrast compared to nitroimidazole-based compounds.[17-19]

In contrast, ^{18}F-FDG retention in cancer cells relies on the increased expression of GLUT-1 and hexokinase-2 to trap the ^{18}F-FDG within the cell.

Hypoxic cells, through stabilized HIF1a, shows increased glycolysis and angiogenesis. Thus ^{18}F-FDG PET imaging can partially reflect hypoxic state of the tumor. In this way, when tumor cells are treated with anti-angiogenesis agents, changes in glycolysis and hypoxia should reflect changes in ^{18}F-FDG and ^{18}F-MISO uptake and distribution.

The purpose of this study is to assess the usefulness of hypoxic radiotracers in anti-angiogenesis therapy in xenograft rodent model.

II. MATERIALS AND METHODS

1. In vitro studies

Colorectal cancer cell lines HCT116, HT29, COLO205 were obtained from the Korean Cell Line Bank. Cell line selection was based on induction of HIF1a under hypoxia conditions and previous studies on bevacizumab (Avastin, Genentech, South San Francisco, CA) therapy response in vivo animal studies.

All cell lines were grown in 5% CO_2 humidified atmosphere at 37^{o}C. Cells were maintained in Roswell Park Memorial Institute medium ((RPMI1640, GIBCO, Grand Island, NY), supplemented with 10% (vol/vol) heat-inactivated fetal bovine serum (FBS) and 1% penicillin and streptomycin (Sigma-Aldrich, P4333). Each cell line was plated in triplicate until 80% confluence. Cells were incubated in 1% O2 hypoxic chamber for 3-4 hours or 12 hours for hypoxic studies. Corresponding cell lines were plated in triplicate and incubated in normoxia chamber (95% air, 5% CO_2 at 37^{o}C) for control. After hypoxic or normoxic condition incubation, these cell lines were incubated with ^{18}F-FDG, or ^{18}F-MISO, or ^{64}Cu-ATSM (2uCi/well for all radiotracers) for one hour in serum free medium for hypoxic radiotracers and in low glucose, serum free medium for ^{18}F-FDG radiotracers. After incubation, all wells were washed three times with 3ml of phosphate buffered saline (PBS), harvested, and cell membrane lysed with cell lysis buffer (Cell Signaling Technology, #9803). Lysates were

counted for radioactivity (PerkinElmer Wallac Wizard 3" 1480 Gamma Counter), centrifuged (12,000 rpm, 20min), after which the pellet was discarded. For ^{64}Cu-ATSM studies, evaluation of dependence of ^{64}Cu-ATSM on various biologic conditions was evaluated. HCT116 cells were incubated with deferoxamine mesylate (DFO) for 8 hours before cell uptake studies.[20] The effect of HIF1a suppression in ^{64}Cu-ATSM uptake was performed by inhibiting HIF1a activation using small interfering RNA (siRNA) was performed according to the protocol supplied by Invitrogen Inc (protocol publication MAN0007824, rev 1.0). Briefly, HIF1a DNA was transfected into cells in 6 well plate using Lipfectamine Reagent in Opti-MEM solution, and incubated for two days at 37C. Then the cells were incubated in either normoxic or hypoxic conditions for either 4 hours and 12 hours, and then incubated with ^{64}Cu-ATSM with the previously mentioned conditions.

Western blot was performed to evaluate for changes in protein expression after hypoxic incubation. Separation of proteins was obtained using sodium dodecyl sulphate polyacrylamide gel electrophoresis (SDS-PAGE). Protein samples for analysis were prepared in accordance with the manufacturer's instructions (Abcam) prior to loading of gels and running in 3-(N-morpholino)propane-sulfonic acid (1×MOPS) running buffer, at 100 V for 1.5 hours. Separated proteins were transferred to a nitrocellulose membrane (Abcam, ab133413) at 100 V for 60 minutes. Membranes were subjected to immunoblotting with mouse monoclonal antibodies to human HIF1a (Cell

Signaling Technology, #3716), or mouse monoclonal antibodies to human GLUT1 (Abcam, ab652) and mouse monoclonal antibodies to β-actin (AC-15, Sigma Chemical Co., Poole, UK) in 1% non-fat milk in phosphate-buffered saline (PBS). This was followed by incubation with horseradish peroxidase-conjugated secondary antibody (goat anti-mouse, from DakoCytomation, Hamburg, Germany, diluted 1:5,000 in 1% non-fat milk and PBS). Proteins were detected by enhanced chemiluminescence (SuperSignal West Pico Chemiluminescent Substrate, Pierce Biotechnology, Rockford, IL, USA) and transparency film.

To evaluate for the effect of extracellular conditions on ^{18}F-MISO retention, ^{18}F-MISO evaluation was performed in cells incubated in acidic culture medium. RPMI media was titrated with lactic acid to change pH to the following levels: 7.8, 7.3, 6.9, 6.7, 6.4, 6.1. HCT116 were grown on 6 well plate and grown to 80% confluence. The media was first removed and then incubated with pH adjusted RPMI into each well plate. Immediately thereafter, 1-2uCi of ^{18}F-MISO was injected into each well plate and incubated for 30 minutes in normoxic conditions. To evaluate for ^{18}F-MISO retention in necrotic cells, HCT116 cells were incubated for 2 hours under intense hyperthermia at 55^{o}C to induce necrosis, in concordance with the methods described in previous studies evaluating radiotracers for tumor necrosis.[21-23] HCT116 cells incubated in normoxia chamber were used as control. Also, to more approximately evaluate in vivo tumor necrosis conditions, HCT116 cell lines were incubated in

prolonged hypoxic chamber (7 days) in FBS-free RPMI media, until media was yellow in color and cells self-detached from well plate. Normoxia and hypoxic conditions were used as control. Cells were scraped, centrifuged, and gamma counted.

2. In vivo studies

A. Tumor model establishment and Avastin therapy

HCT116 cell line was cultured and $1.0x10^6$ cells/100uL in PBS was subcutaneously injected into the right hind leg of 64 BALB/c-nu Slc mice weighing 20g on average. Tumor growth was calculated with digital caliper. When the tumors grew to approximately 1.5-2cm, pre-therapy PET images were acquired and anti-angiogenesis therapy started. The mice were grouped into treatment group and control group. All animal experiments followed the ethical committee of the Yonsei University of Animal Care and Use. The treatment group was injected intraperitoneally with 10mg/kg of Avastin, two times a week for two weeks. Control group received intraperitoneal normal saline injections of 200ul. Tumor response to Avastin therapy was determined by tumor size growth ($(a*b^2)/2$; a: long side, b: short side) and by immunohistochemical analysis.

B. Animal Positron Emission Tomography (microPET) and autoradiography protocol

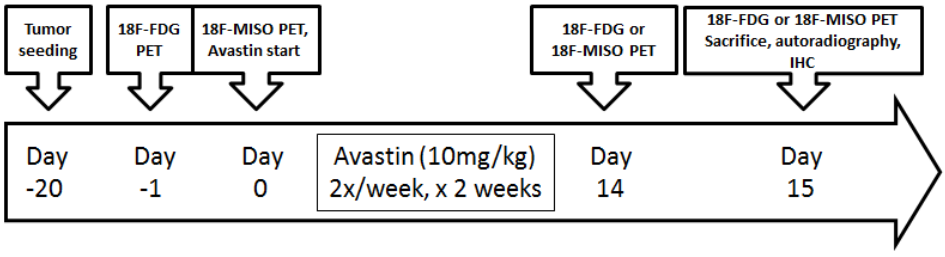

Figure 1. Timeline of Avastin therapy for hypoxic radiotracer assessment

PET imaging schedule was as follows: ^{18}F-FDG PET was acquired one day before therapy. On the day of therapy, ^{18}F-MISO was acquired before Avastin administration (Figure 1). Approximately 200uCi of ^{18}F-FDG or ^{18}F-MISO was injected intravenously, and PET images were acquired 60 minutes later for ^{18}F-FDG PET, and 2 hours later for ^{18}F-MISO PET. Animals were ventilated with an isoflurane/air mixture (1% isoflurane). Mice were fasted for at least 8 hours before ^{18}F-FDG PET images. A 10 min PET scan was acquired using an Inveon PET (Siemens Medical Solutions, Knoxville, KY, USA). After data acquisition, PET data was arranged into sinograms and subsequently reconstructed with the maximum a posteriori (MAP) reconstruction algorithm. After two weeks of Avastin therapy, ^{18}F-FDG and ^{18}F-MISO PET images were acquired before sacrifice. Pimonidazole solution (60 mg/kg in 100ul normal

saline; Hypoxyprobe-1 kit; Hypoxyprobe, Inc., Burlington, MA, USA) was injected intraperitoneally 2 hours before sacrifice. To acquire ^{18}F-FDG autoradiography images, 11 mice of the control group and 11 mice of the therapy group were randomly chosen to have ^{18}F-MISO PET a day before sacrifice, and had ^{18}F-FDG PET on the day of sacrifice. To acquire ^{18}F-MISO autoradiography images, 11 mice of the control group, and 11 mice of the therapy group had ^{18}F-FDG PET a day before sacrifice and ^{18}F-MISO PET on the day of sacrifice. Immediately after PET acquisition, the mice were sacrificed; tumors were excised, and cut in half. One half was put into 10% formaldehyde and half was frozen in -70C with Tissue-Tek O.C.T Compound (Sakura Finetek Europe B.V.). The thigh muscles of the non-tumor bearing leg were also excised and included in the frozen tumor block and used as reference for radiotracer uptake in autoradiography slides. The frozen tumors were immediately cryosectioned with cryomicrotome (CM1860, LEICA, Nussloch, Deutschland) at 8um slice thickness on five frosted microscope slides, and autoradiography images were acquired with imaging plate (BAS-SR 2040; Fujifilm, Tokyo, Japan). The imaging plate was then scanned with a bio-imaging analyzer (FLA7000; Fujifilm, Tokyo, Japan).

^{64}Cu-ATSM studies performed using the same imaging protocol and timeline as Figure 1, with ^{64}Cu-ATSM microPET acquired instead of ^{18}F-MISO. Twenty mice underwent baseline 18F-FDG and 64Cu-ATSM microPET, after which 10 mice had Avastin therapy, and 10 mice were control group. After

therapy, all mice underwent 18F-FDG microPET one day before sacrifice and then ^{64}Cu-ATSM microPET on the day of sacrifice. Tumors were excised, and all tumors had ^{64}Cu-ATSM autoradiography after cryosection.

C. Histopathology and Imaging Analysis

MicroPET images were reviewed using PMOD software (version 3.6). Three circular or elliptical region of interests (ROIs) of 1mm were drawn on the PET images manually on the areas with high radiotracer uptake in the tumors and the maximum standard uptake value (SUVmax) was recorded. For mean standard uptake value (SUVmean), the average of the SUVmean within the three ROI was used. Muscle uptake in the leg contralateral to the tumor bearing leg was used for reference, and three similar ROIs were drawn and SUVmean was used as reference. The tumor-to-muscle ratio was used for quantitative analysis. To evaluate for radiotracer uptake in necrotic components, the autoradiography images were used. Using Multi Gauge software (Fujifilm, Tokyo, Japan), three ROIs were drawn on the necrotic areas, using the corresponding hematoxylin and eosin (H&E) slides for reference, and the average PSL/mm values were recorded. Three ROIs of the muscle in the autoradiography was used for reference tissue uptake. The ratio between lesion-to-muscle uptake was used for quantitative analysis.

Treatment and control groups was stained with H&E, hypoxyprobe-1

Mab1 (monoclonal antibody used to detect pimonidazole adducts), and Ki-67 (Abcam, ab15580). The pathology slides were digitally scanned at 400x resolution. The necrotic portions were determined using H&E staining.[24] Quantification of pathology slides was performed using ImageJ software, and percent area was used for quantification. Hypoxic area was analyzed using pimonidazole staining. Therapy response was evaluated by comparing % area of necrosis, hypoxic components, and Ki-67 positivity over the whole tumor.

III. Results

1. In vitro studies

Colon cancer cell lines HCT116, HT29, Colo205 were incubated in 1% hypoxic chamber for 3 hours or 12~15 hours and compared with normoxic conditions. All cell lines showed higher ^{18}F-MISO and ^{18}F-FDG retention in hypoxic conditions compared to normoxic conditions. HCT116 showed highest ratio of ^{18}F-MISO retention in hypoxic conditions compared to normoxic conditions (3 hour: 6.5, 12 hour: 5.1, Figure 2a). Western blot analysis showed the highest induction of HIF1a in HCT116, and lesser induction in HT29 cell line, and the least induction in Colo205 in hypoxic conditions compared to normoxic conditions (Figure 2b). Minimal GLUT1 induction was seen in all cell lines for the 3 hour and 12 hour hypoxic incubation times. Interestingly, Colo205 showed relatively high ^{18}F-FDG uptake after hypoxic induction, but low ^{18}F-MISO uptake. Western blot analysis also showed minimal HIF1a induction, but relatively stronger induction of GLUT1 in hypoxic conditions. Based on these results, HCT116 was selected for in vivo studies.

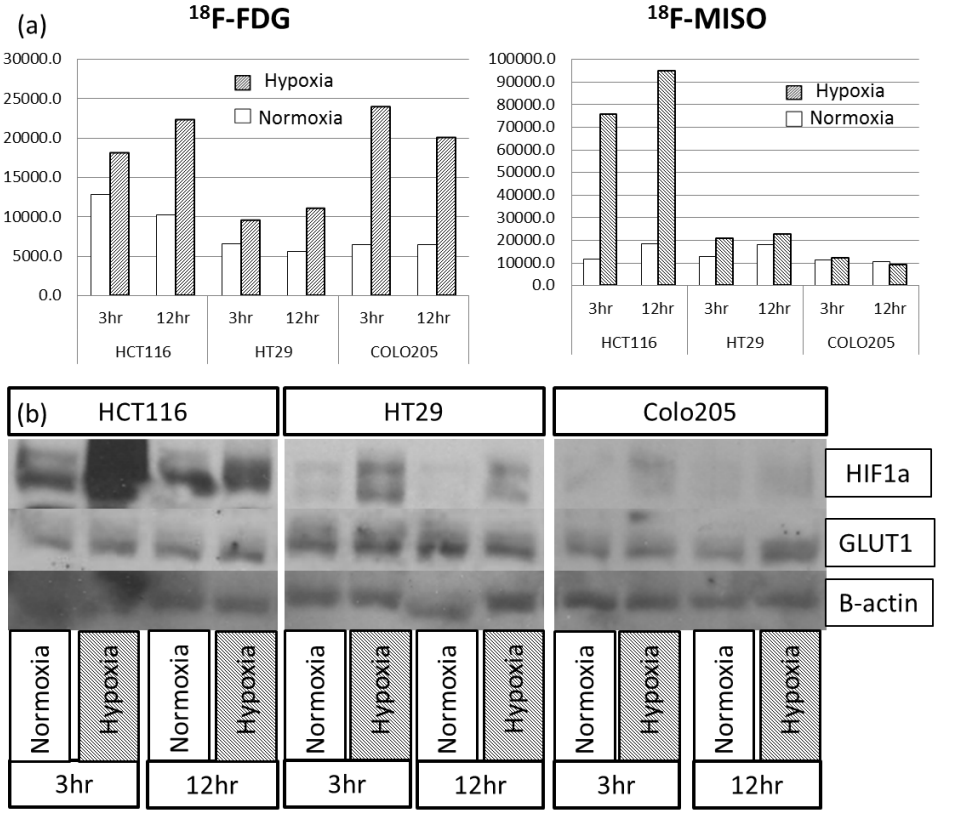

Figure 2. In vitro radiotracer uptake study and western blot analysis in various tumor cell lines. (a) Compared to normoxic conditions, all cell lines showed increase in ^{18}F-FDG and ^{18}F-MISO uptake after 3 hour and 12 hour hypoxia induction. (b) Western blot analysis showed highest HIF1a induction in HCT116 cell line, then HT29, and least amount in Colo205. Minimal GLUT1 induction is seen in all cell lines after hypoxic induction.

2. In vivo studies

A. Evaluation of therapy response to Avastin in HCT116 cell lines

HCT116 was inoculated in right flank of the mice, and Avastin therapy was performed approximately when the tumors were grown to 1.5cm, and tumors were excised after 20 days of therapy. Figure 3 shows signification inhibition of tumor growth after Avastin therapy. Eleven tumor specimens from the control group and twenty tumor specimens from the treatment group were excised and stained with H&E, pimonidazole, and Ki-67 for treatment response evaluation. There was no significant difference in necrotic components or Ki-67 expression between the control group and therapy group (Table 1). However, there was a significant increase in hypoxic area in the treatment group compared to the control group (control group: 49.33% ± 11.84, treatment group: 41.69 ± 22.58, p=0.328, t-test).

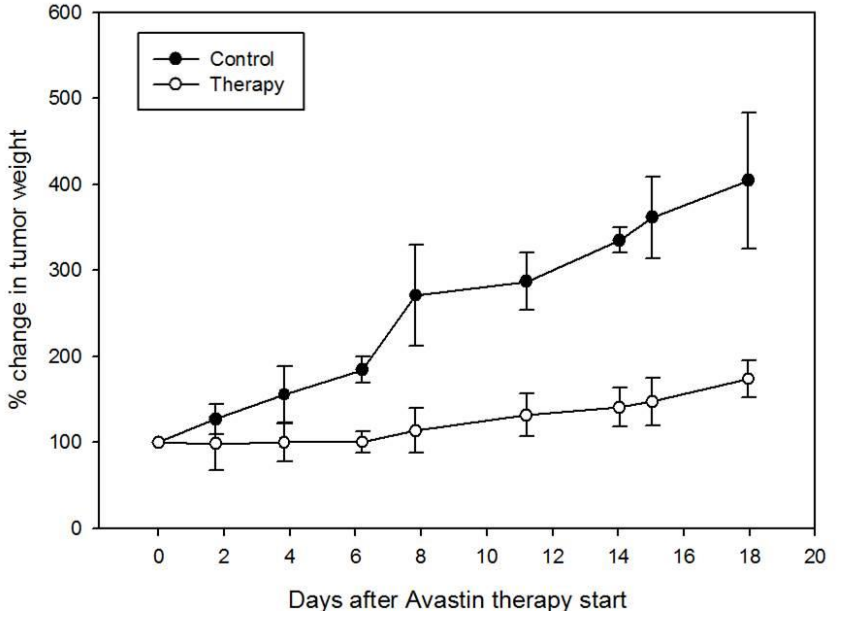

Figure 3. Tumor growth delay curve. Avastin therapy group showed tumor growth delay compared to control group.

Table 1. Comparison of immunohistologic changes after Avastin treatment in HCT 116 colon cancer cell line.

	Viable portion (%area)	**Hypoxia portion (%area)**	**Ki67 (%area)**	**Necrotic (%area)**
Control (n=11)	72.18 ± 14.0	11.02 ± 4.81	49.33 ± 13.84	27.82 ± 14
Treatment (n=20)	63.98 ± 24.8	17.67 ± 5.95	41.69 ± 22.58	36.02 ± 24.8
p-value	0.249	**0.004**	0.328	0.249

MicroPET images after Avastin therapy were evaluated for differences in ^{18}F-FDG or ^{18}F-MISO uptake in the control group compared to treatment group. There was no significant difference in SUVmax or SUVmean between the treatment or control group (Table 2).

Table 2. Comparison of ^{18}F-FDG and ^{18}F-MISO uptake in control and treatment groups

	^{18}F-FDG			**^{18}F-MISO**		
	N	**SUVmax***	**SUVmean ****	**N**	**SUVmax ***	**SUVmean ****
Control	19	3.0 ± 1.8	2.8 ± 1.6	11	4.6 ± 2.7	4 ± 2.6
Treatment	13	5.4 ± 6.4	3.2 ± 1.9	9	4.6 ± 3.0	3.9 ± 2.5
p-value		0.123	0.48		0.953	0.972

*lesion/muscle ratio

**SUL (1mm)

B. Evaluation of ^{18}F-MISO retention in necrotic tumors

However, visual analysis showed that in tumors with necrotic components, ^{18}F-FDG showed photon defect in the central portion of the tumor, but ^{18}F-MISO showed mild diffuse uptake in the center portion (Figure 4). Quantitative analysis using available ^{18}F-FDG and ^{18}F-MISO autoradiography showed significantly higher ^{18}F-MISO uptake in the necrotic portions compared to ^{18}F-FDG (Table 3). Corresponding H&E slides showed necrotic

cells in the area that showed photon defect in ^{18}F-FDG PET and increased uptake in the ^{18}F-MISO PET (Figure 5).

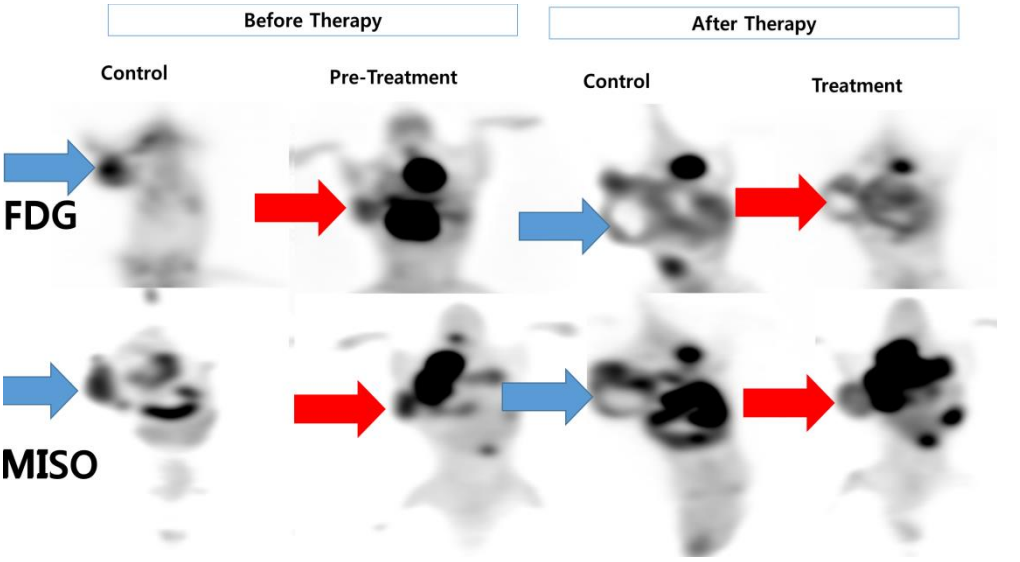

Figure 4. MicroPET scan showing uptake patterns in HCT116 tumors after Avastin therapy. In post-therapy PET images, there was a mismatch between ^{18}F-FDG and ^{18}F-MISO uptake in the tumor center.

Table 3. Comparison of hypoxic radiotracer retention in necrotic portions

Radiotracer	Viable portion*	Necrotic portion*
^{18}F-FDG (n=31)	2.99±1.74	0.83±0.42††
^{18}F-MISO (n=10)	3.95±2.47†	2.41±1.77††,‡
^{64}Cu-ATSM (n=10)	2.37±0.76†	0.94±0.48‡

***lesion/muscle ratio; †p=0.092 ; ††p=0.001 ; ‡ p=0.005**

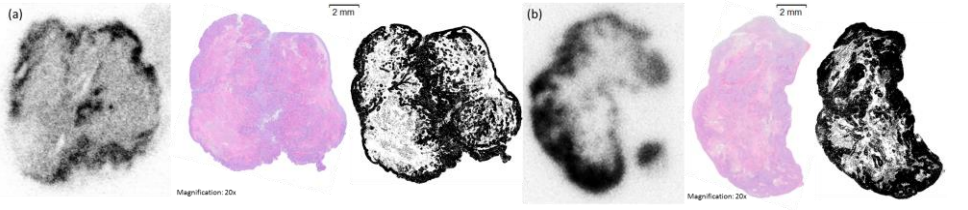

Figure 5. ^{18}F-MISO and ^{18}F-FDG autoradiography with corresponding H&E pathology slides. (a) Post therapy ^{18}F-MISO autoradiography shows mild diffuse uptake within the necrotic components seen on corresponding pathology slide. (b) post therapy ^{18}F-FDG autoradiography showed minimal uptake in the necrotic portions seen on corresponding pathology slide.

3. In vitro studies in dependence of ^{18}F-MISO uptake according to pH and necrosis

A. Dependence of ^{18}F-MISO uptake in pH and tumor acidity

Lactic acid was added to RPMI media until pH of the media showed the changes in pH that is seen in Figure 6. The original media incubating HCT116 was removed, and the pH adjusted media was administered to these cell lines. 1-2uCi of ^{18}F-MISO was immediately added, and incubation for 30 minutes was given for intracellular uptake. Then the media was removed, PBS washed three

times, and radiotracer uptake in these cells was counted. Figure 6 shows the changes in ^{18}F-MISO uptake compared to pH 7.8. When pH was dropped to lower to 6.9, the intracellular ^{18}F-MISO uptake was reduced to 50~60% compared to cells that were incubated at pH of 7.8 (Figure 6).

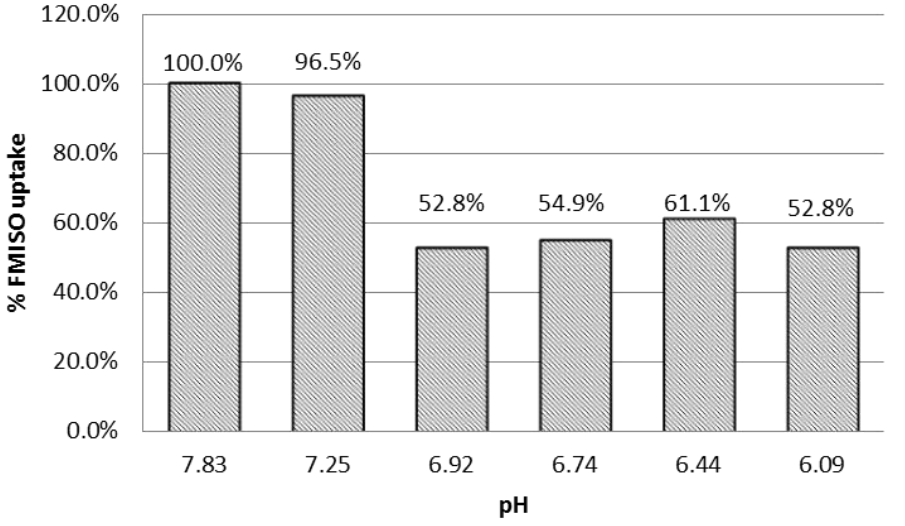

Figure 6. Dependence of ^{18}F-MISO uptake on extracellular pH. Reduction of ^{18}F-MISO uptake is seen in pH lower than 6.9

B. in vitro evaluation of ^{18}F-MISO uptake in necrotic cells

To determine the ^{18}F-MISO uptake in necrotic cells, HCT116 cells were incubated in various conditions known to induce necrosis. Necrosis was induced either by incubation in high temperatures (55^{o}C) for two hours, or incubated in serum free media in hypoxic chamber for prolonged period (6 days).[21-23,25] Then,

^{18}F-MISO was administered and radioactivity determined. ANOVA analysis showed a significant difference in ^{18}F-MISO uptake in heat necrotic and hypoxic cells compared to normoxia cells (Figure 7).

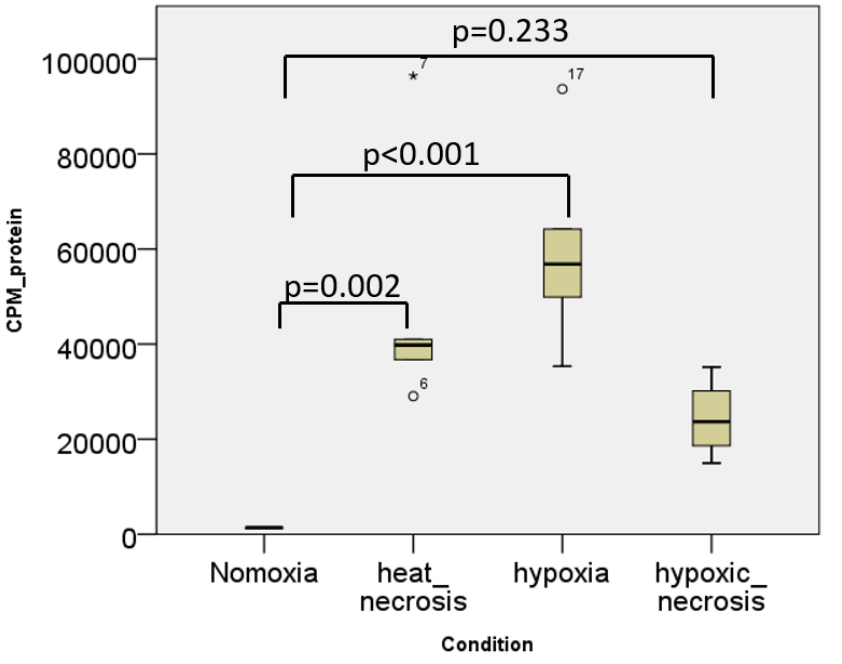

Figure 7. Comparison of ^{18}F-MISO retention in necrotic conditions compared to hypoxic or normoxic HCT116 cells. Significant difference in ^{18}F-MISO retention is seen in heat necrosis and hypoxic cells compared to normoxic cells.

4. In vitro and in vivo studies using ^{64}Cu-ATSM

A. in vitro study

^{64}Cu-ATSM was incubated with the same method as ^{18}F-MISO. ^{64}Cu-ATSM showed approximately 3 times higher radiotracer uptake in hypoxic conditions (3.3 times higher at 4 hours and 2.8 higher at 12hours) compared to normoxic conditions. (Figure 8a). After cells were incubated in DFO to prevent HIF1a from degrading, the ^{64}Cu-ATSM uptake ratio did not change as much (3.7 times higher for 4-hour hypoxic incubation, and 2.2 times higher for 12-hour hypoxic incubation). There was minimal effect on ^{64}Cu-ATSM uptake after HIF1a inhibition using siRNA as well (2.2 higher uptake after 4-hour hypoxic incubation, and 3.4 times higher uptake after 12-hour incubation). Western blot analysis shows increased expression of HIF1a after hypoxia induction at 4 hours and 12 hours, with higher expression at 4 hours compared to 12-hour incubation (Figure 8b). Western blot analysis shows siRNA induced HIF1a inhibition.

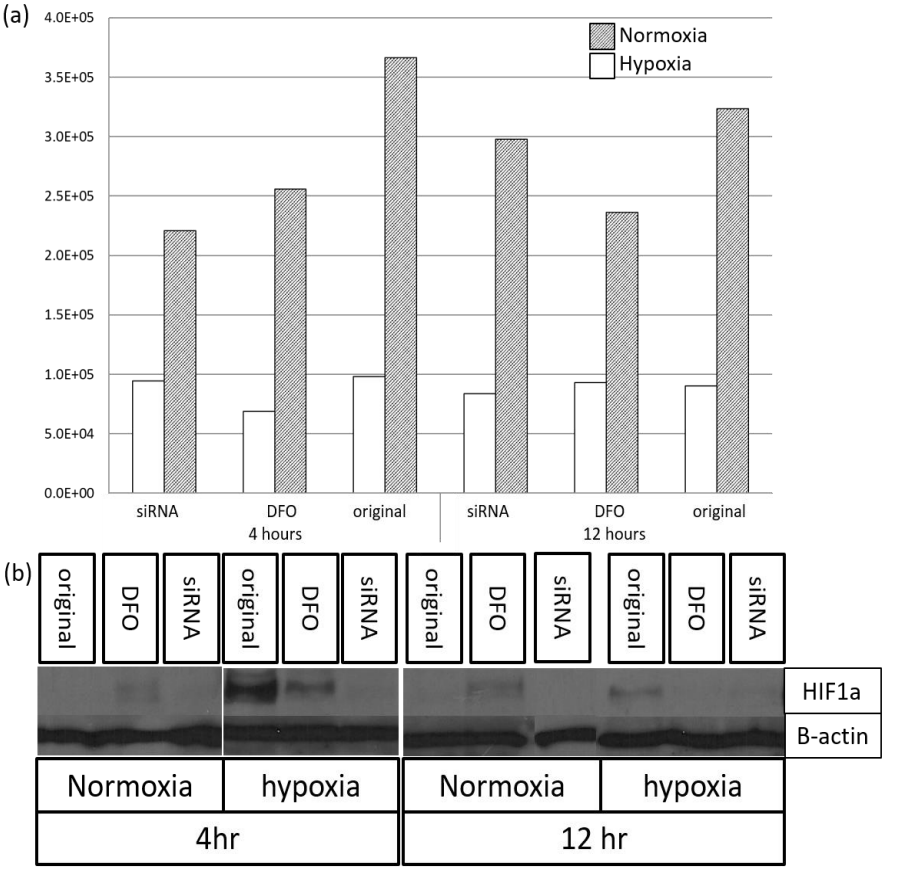

Figure 8. Evaluation of ^{64}Cu-ATSM uptake in various hypoxic (1%) and biologic conditions. (a) Comparison of ^{64}Cu-ATSM uptake in various biologic conditions. (b) western blot analysis of cells incubated after 4-hour and 12-hour hypoxic chamber incubation for HCT116 cells after HIF1a stabilization with DFO or HIF1a expression suppression with siRNA.

B. in vivo study

In contrast to ^{18}F-MISO, ^{64}Cu-ATSM showed minimal radiotracer uptake in the necrotic portions of the tumor (Figure 9). Autoradiography analysis showed no significant difference in ^{64}Cu-ATSM uptake in the necrotic components compared to ^{18}F-FDG (Table 3).

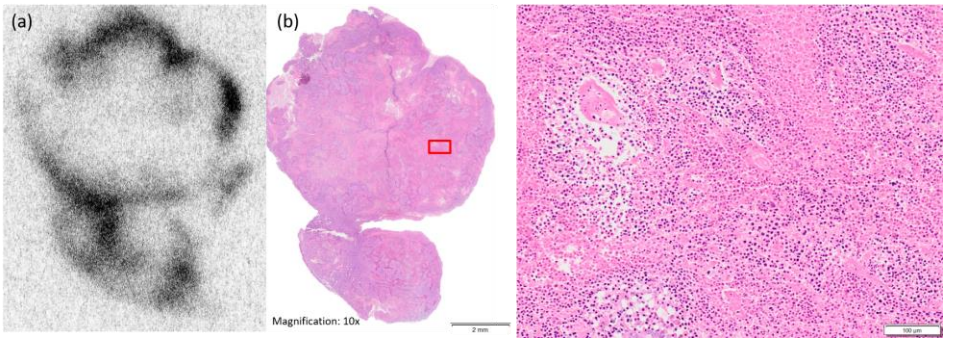

Figure 9. ^{64}Cu-ATSM autoradiography of HCT116 tumor with necrotic components (a) ^{64}Cu-ATSM autoradiography reveals minimal radiotracer uptake in the central necrotic portions. (b) H&E slide shows near total necrosis in this area.

IV. DISCUSSION

Antiangiogenic therapy combined with standard chemotherapy improves therapy response and survival in metastatic colorectal cancer.[26] However, other studies have suggested poorer prognosis in adjuvant chemotherapy in stage II, III colon cancers.[27,28] Recent studies have suggested that antiangiogenic therapy causes accelerated metastasis or increased local invasion, suggesting adaptive resistance to anti-angiogenetic therapy.[29-32] These results suggest an increased importance of developing a imaging method to serially evaluate changes in hypoxia and anti-angiogenesis therapy.[33,34] We have shown in our study of HCT116 human colon cancer cell line subcutaneous xenograft murine model that tumor growth suppression was seen after two weeks of Avastin therapy, which was also in concordance with various studies using Avastin in tumor growth suppression in animal studies.[4,35-43] Pimonidazole immunohistologic slides revealed an increase in hypoxic areas in the Avastin treated tumors compared to control tumors. This is also in concordance with a previous study evaluating Avastin therapy response in HCT116 tumors. Selvakumaran et al has shown that after short term Avastin therapy, microvessel density is decreased, resulting in increase in hypoxic areas.[36] Interestingly, we have seen that there was no significant difference in relative necrotic portions between the treatment group and control group. This may be due to the slower tumor growth in Avastin treated tumors, resulting in smaller areas of tumor necrosis.

We have compared the ^{18}F-FDG uptake changes in hypoxic conditions with ^{18}F-MISO in various colon cancer cell lines. We have confirmed that glycolysis is increased in hypoxic conditions, but the amount of increase is not as high as ^{18}F-MISO, which suggests that ^{18}F-MISO reflects hypoxic changes better than ^{18}F-FDG. We have also shown that despite HIF1a degradation in prolonged hypoxia (15hours) ^{18}F-MISO retention is persistently high, which also suggests that ^{18}F-MISO may be a better marker for hypoxia in in vivo conditions, as previous studies have shown that prolonged hypoxia has been shown to degrade HIF1a.[44] Initial comparison of colon cancer cell lines revealed that 18F-MISO retention in hypoxic conditions was lower in HT29 and COLO205 cell lines compared to HCT116. Although further investigations were not performed, one possible theory maybe the difference in expression of nitroreductase enzymes between these cell lines. However, due to the myriad of different nitroreductase enzymes expressed in cancer cells, it may not be easily feasible to correlate between nitroreductase enzyme expression with ^{18}F-MISO retention.

In the evaluation of post-therapy PET images to evaluate for therapy response to Avastin in HCT116, generally we have seen a mismatch of ^{18}F-FDG uptake and ^{18}F-MISO uptake in larger tumors. Larger subcutaneous tumors generally form necrotic core, which shows photon defect in ^{18}F-FDG PET images. However, ^{18}F-MISO PET shows mild uptake in these necrotic portions, with uptake intensity similar to the skeletal muscle uptake in the

contralateral leg muscles. Although the viable portions of the tumor show significantly high ^{18}F-MISO uptake, this mild uptake in the center may be misleading if ^{18}F-FDG PET was not acquired for comparison of uptake distribution. Semiquantitative analysis using a ratio between tumor to muscle uptake showed no significant difference in ^{18}F-MISO uptake in the viable portions of the tumor. ^{18}F-FDG uptake was slightly higher in the treated tumors, but this was not significant.

To further evaluate for this ^{18}F-MISO retention in necrotic portions, the autoradiography images were analyzed, using the H&E images for reference to determine the necrotic portions of the tumor. Autoradiography images were used instead of PET images due to the relative high spatial resolution of autoradiography images (<200um) compared to microPET images, and also the corresponding H&E slides provide a general map of necrotic portions on the tumor. There was a significant higher retention of ^{18}F-MISO in the necrotic portions of the tumor compared to ^{18}F-FDG. Despite the extensive studies on ^{18}F-MISO, there are only a few studies that have mentioned ^{18}F-MISO retention in necrotic portions of tumors. Of those, a group by Huang et al have shown a similar ratio between muscle and tumor necrosis uptake in their results.[45,46] In contrast, another group has found no correlation between tumor to muscle radioactivity uptake with necrotic fraction in their study using C3H mammary carcinomas.[24]

To further evaluate the possible mechanisms for the retention of

^{18}F-MISO in tumor necrosis, in vitro studies were performed. Nitroimidazole compounds differ from most other radiotracers in that the nitroimidazole ring is pH sensitive. Of the two nitrogen atoms in the nitroimidzaole ring, one is substituted with a side chain that contains the F-18 isotope. The other nitrogen is not substituted, which allows it to be protonated. The pKa of this nitrogen is known to be approximately 7.1,[47] and studies have shown that in vivo, the extracellular fluid in tumors are more acidic (pH=6.9) compared to normal tissues (pH=7.4).[48-57] A recent study has shown that this lowered pH in tumors may affect transport of pH sensitive drugs into the cell. Doxirubicin is also protonated in acidic environments, which reduces the intracellular concentrations of Doxirubicin in tumors compared to normal tissues.[58] Likewise, ^{18}F-MISO may also be affected by the extracellular pH. Our preliminary results suggests reduced ^{18}F-MISO uptake in culture media with pH lower than 6.9. However, further studies are needed to fully evaluate whether this protonated ^{18}F-MISO may be a factor for ^{18}F-MISO retention in necrotic portions of the tumor. Another possible mechanism for ^{18}F-MISO retention in the necrotic area is the high lipophilicity of ^{18}F-MISO compound. Unlike ^{18}F-DG, which requires GLUT transporter to transport into the cell, ^{18}F-MISO high lipophilicity (log P=0.4),[47] suggests easy permeability across the lipid membrane, and any functional nitroreductase may cause ^{18}F-MISO to be inadvertently trapped within the cell. Our results suggest some ^{18}F-MISO retention in necrotic tumor cells in vitro. Further studies are needed to fully

validate these results. Other possible mechanisms are the poor vascularity, in which the ^{18}F-MISO may be delivered slowly with slow washout. ^{18}F-MISO metabolite studies and kinetic analysis of dynamic PET scans are needed to discern whether ^{18}F-MISO uptake in the necrotic portions is due to delivery or metabolism differences.

Despite ^{18}F-MISO showing excellent retention in hypoxic conditions, retention of ^{18}F-MISO in necrotic portions suggest that it may not be optimal tracer in the clinical setting, especially in the evaluation of hypoxic status in patients who underwent chemotherapy or radiotherapy. ^{18}F-MISO retention, although mild could affect reader ability to determine hypoxic status of these necrotic tumors, or may mask the subtle uptakes in viable, but hypoxic tumors, or may be an impediment in evaluating viable, non-hypoxic tumors. Therefore, further investigations using another hypoxic radiotracer, ^{64}Cu-ATSM was performed. In contrast to ^{18}F-MISO, ^{64}Cu-ATSM retention mechanism relies on electron transport chain to reduce the radioactive copper, lowering its affinity from the ATSM chelate. Cu-64 will be then trapped within the cell, which will then be visualized by PET. ^{64}Cu-ATSM is not pH sensitive, and is less lipophilic compared to ^{18}F-MISO, which allows for shorter interval between injection and PET scanning. Initial in vitro results showed similar high retention of ^{64}Cu-ATSM in hypoxic conditions compared to normoxic conditions. Also, to evaluate the independence of ^{64}Cu-ATSM retention with the biologic response to hypoxia, HIF1a silencing with siRNA showed

persistent high retention of ^{64}Cu-ATSM in hypoxic conditions even after HIF1a suppression. In vivo studies also showed that ^{64}Cu-ATSM retention in necrotic portions are similar to ^{18}F-FDG studies, and was significantly lower compared to ^{18}F-MISO. These results suggest that in tumors with necrotic portions, ^{64}Cu-ATSM may be a better radiotracer to evaluate tumor hypoxia than ^{18}F-MISO.

V. CONCLUSION

In subcutaneous tumor model for HCT116 colon cancer cell line, significant tumor growth suppression is seen after two weeks of Avastin therapy, as well as an increase in hypoxic area. In tumors with necrotic portions, ^{64}Cu-ATSM PET may reflect non-viable portions better than ^{18}F-MISO PET. A possible mechanism for increased retention of ^{18}F-MISO in necrotic portions in tumors may be due to the lipophilicity of ^{18}F-MISO or the pH sensitive components of the nitroimidazole ring of ^{18}F-MISO.

REFERENCES

1. Hanahan D, Weinberg RA. The hallmarks of cancer. Cell 2000;100:57-70.
2. Rajendran JG, Krohn KA. Imaging hypoxia and angiogenesis in tumors. Radiol Clin North Am 2005;43:169-87.
3. Vaupel P, Harrison L. Tumor hypoxia: causative factors, compensatory mechanisms, and cellular response. Oncologist 2004;9 Suppl 5:4-9.
4. Jain RK. Tumor angiogenesis and accessibility: role of vascular endothelial growth factor. Semin Oncol 2002;29:3-9.
5. Iqbal S, Lenz HJ. Angiogenesis inhibitors in the treatment of colorectal cancer. Semin Oncol 2004;31:10-6.
6. Ou G, Itasaka S, Zeng L, Shibuya K, Yi J, Harada H, et al. Usefulness of HIF-1 imaging for determining optimal timing of combining bevacizumab and radiotherapy. Int J Radiat Oncol Biol Phys 2009;75:463-7.
7. Harada H, Kizaka-Kondoh S, Itasaka S, Shibuya K, Morinibu A, Shinomiya K, et al. The combination of hypoxia-response enhancers and an oxygen-dependent proteolytic motif enables real-time imaging of absolute HIF-1 activity in tumor xenografts. Biochem Biophys Res Commun 2007;360:791-6.
8. Harada H, Kizaka-Kondoh S, Hiraoka M. Optical imaging of tumor hypoxia and evaluation of efficacy of a hypoxia-targeting drug in living animals. Mol Imaging 2005;4:182-93.
9. Dings RP, Loren M, Heun H, McNiel E, Griffioen AW, Mayo KH, et al. Scheduling of radiation with angiogenesis inhibitors anginex and Avastin improves therapeutic outcome via vessel normalization. Clin Cancer Res 2007;13:3395-402.
10. Eschmann SM, Paulsen F, Reimold M, Dittmann H, Welz S, Reischl G, et al. Prognostic impact of hypoxia imaging with 18F-misonidazole PET in non-small cell lung cancer and head and neck cancer before radiotherapy. J Nucl Med 2005;46:253-60.
11. Rajendran JG, Schwartz DL, O'Sullivan J, Peterson LM, Ng P, Scharnhorst J, et al. Tumor hypoxia imaging with [F-18] fluoromisonidazole positron emission tomography in head and neck cancer. Clin Cancer Res 2006;12:5435-41.
12. Thorwarth D, Eschmann SM, Holzner F, Paulsen F, Alber M. Combined uptake of [18F]FDG and [18F]FMISO correlates with radiation therapy outcome in head-and-neck cancer patients. Radiother Oncol 2006;80:151-6.
13. Kizaka-Kondoh S, Konse-Nagasawa H. Significance of nitroimidazole compounds and hypoxia-inducible factor-1 for imaging tumor hypoxia. Cancer Sci 2009;100:1366-73.
14. Anderson CJ, Ferdani R. Copper-64 radiopharmaceuticals for PET

imaging of cancer: advances in preclinical and clinical research. Cancer Biother Radiopharm 2009;24:379-93.
15. Burgman P, O'Donoghue JA, Lewis JS, Welch MJ, Humm JL, Ling CC. Cell line-dependent differences in uptake and retention of the hypoxia-selective nuclear imaging agent Cu-ATSM. Nucl Med Biol 2005;32:623-30.
16. Dence CS, Ponde DE, Welch MJ, Lewis JS. Autoradiographic and small-animal PET comparisons between (18)F-FMISO, (18)F-FDG, (18)F-FLT and the hypoxic selective (64)Cu-ATSM in a rodent model of cancer. Nucl Med Biol 2008;35:713-20.
17. Hansen AE, Kristensen AT, Jorgensen JT, McEvoy FJ, Busk M, van der Kogel AJ, et al. (64)Cu-ATSM and (18)FDG PET uptake and (64)Cu-ATSM autoradiography in spontaneous canine tumors: comparison with pimonidazole hypoxia immunohistochemistry. Radiat Oncol 2012;7:89.
18. Lewis JS, McCarthy DW, McCarthy TJ, Fujibayashi Y, Welch MJ. Evaluation of 64Cu-ATSM in vitro and in vivo in a hypoxic tumor model. J Nucl Med 1999;40:177-83.
19. Lewis JS, Sharp TL, Laforest R, Fujibayashi Y, Welch MJ. Tumor uptake of copper-diacetyl-bis(N(4)-methylthiosemicarbazone): effect of changes in tissue oxygenation. J Nucl Med 2001;42:655-61.
20. Hervouet E, Cizkova A, Demont J, Vojtiskova A, Pecina P, Franssen-van Hal NL, et al. HIF and reactive oxygen species regulate oxidative phosphorylation in cancer. Carcinogenesis 2008;29:1528-37.
21. Wang C, Jin Q, Yang S, Zhang D, Wang Q, Li J, et al. Synthesis and Evaluation of 131I-Skyrin as a Necrosis Avid Agent for Potential Targeted Radionuclide Therapy of Solid Tumors. Mol Pharm 2016;13(1):180-189.
22. Van de Putte M, Ni Y, De Witte PA. Exploration of the mechanism underlying the tumor necrosis avidity of hypericin. Oncol Rep 2008;19:921-6.
23. Perek N, Sabido O, Le Jeune N, Prevot N, Vergnon JM, Clotagatide A, et al. Could 99mTc-glucarate be used to evaluate tumour necrosis? In vitro and in vivo studies in leukaemic tumour cell line U937. Eur J Nucl Med Mol Imaging 2008;35:1290-8.
24. Gronroos T, Bentzen L, Marjamaki P, Murata R, Horsman MR, Keiding S, et al. Comparison of the biodistribution of two hypoxia markers [18F]FETNIM and [18F]FMISO in an experimental mammary carcinoma. Eur J Nucl Med Mol Imaging 2004;31:513-20.
25. Jiang B, Wang J, Ni Y, Chen F. Necrosis avidity: a newly discovered feature of hypericin and its preclinical applications in necrosis imaging. Theranostics 2013;3:667-76.
26. Sparano JA, Gray R, Giantonio B, O'Dwyer P, Comis RL. Evaluating

antiangiogenesis agents in the clinic: the Eastern Cooperative Oncology Group Portfolio of Clinical Trials. Clin Cancer Res 2004;10:1206-11.
27. Sargent DJ. Chemotherapy: Failure of bevacizumab in early-stage colon cancer. Nat Rev Clin Oncol 2011;8:10-1.
28. Allegra CJ, Yothers G, O'Connell MJ, Sharif S, Petrelli NJ, Colangelo LH, et al. Phase III trial assessing bevacizumab in stages II and III carcinoma of the colon: results of NSABP protocol C-08. J Clin Oncol 2011;29:11-6.
29. Bergers G, Hanahan D. Modes of resistance to anti-angiogenic therapy. Nat Rev Cancer 2008;8:592-603.
30. Wenger JB, Santos N, Liu Y, Dallas J, Subbiah S, Hochwald S, et al. Can we develop effective combination antiangiogenic therapy for patients with hepatocellular carcinoma? Oncol Rev 2011;5:177-84.
31. Ebos JM, Lee CR, Cruz-Munoz W, Bjarnason GA, Christensen JG, Kerbel RS. Accelerated metastasis after short-term treatment with a potent inhibitor of tumor angiogenesis. Cancer Cell 2009;15:232-9.
32. Paez-Ribes M, Allen E, Hudock J, Takeda T, Okuyama H, Vinals F, et al. Antiangiogenic therapy elicits malignant progression of tumors to increased local invasion and distant metastasis. Cancer Cell 2009;15:220-31.
33. Jain RK, Duda DG, Willett CG, Sahani DV, Zhu AX, Loeffler JS, et al. Biomarkers of response and resistance to antiangiogenic therapy. Nat Rev Clin Oncol 2009;6:327-38.
34. Sandler AB, Schiller JH, Gray R, Dimery I, Brahmer J, Samant M, et al. Retrospective evaluation of the clinical and radiographic risk factors associated with severe pulmonary hemorrhage in first-line advanced, unresectable non-small-cell lung cancer treated with Carboplatin and Paclitaxel plus bevacizumab. J Clin Oncol 2009;27:1405-12.
35. Yanagisawa M, Fujimoto-Ouchi K, Yorozu K, Yamashita Y, Mori K. Antitumor activity of bevacizumab in combination with capecitabine and oxaliplatin in human colorectal cancer xenograft models. Oncol Rep 2009;22:241-7.
36. Selvakumaran M, Yao KS, Feldman MD, O'Dwyer PJ. Antitumor effect of the angiogenesis inhibitor bevacizumab is dependent on susceptibility of tumors to hypoxia-induced apoptosis. Biochem Pharmacol 2008;75:627-38.
37. Jahnke K, Muldoon LL, Varallyay CG, Lewin SJ, Kraemer DF, Neuwelt EA. Bevacizumab and carboplatin increase survival and asymptomatic tumor volume in a glioma model. Neuro Oncol 2009;11:142-50.
38. Huynh H, Chow PK, Palanisamy N, Salto-Tellez M, Goh BC, Lee CK, et al. Bevacizumab and rapamycin induce growth suppression in mouse models of hepatocellular carcinoma. J Hepatol 2008;49:52-60.
39. Huynh H, Teo CC, Soo KC. Bevacizumab and rapamycin inhibit tumor

growth in peritoneal model of human ovarian cancer. Mol Cancer Ther 2007;6:2959-66.
40. Bozec A, Sudaka A, Fischel JL, Brunstein MC, Etienne-Grimaldi MC, Milano G. Combined effects of bevacizumab with erlotinib and irradiation: a preclinical study on a head and neck cancer orthotopic model. Br J Cancer 2008;99:93-9.
41. Schicher N, Paulitschke V, Swoboda A, Kunstfeld R, Loewe R, Pilarski P, et al. Erlotinib and bevacizumab have synergistic activity against melanoma. Clin Cancer Res 2009;15:3495-502.
42. Bauerle T, Bartling S, Berger M, Schmitt-Graff A, Hilbig H, Kauczor HU, et al. Imaging anti-angiogenic treatment response with DCE-VCT, DCE-MRI and DWI in an animal model of breast cancer bone metastasis. Eur J Radiol 2010;73:280-7.
43. Rapisarda A, Hollingshead M, Uranchimeg B, Bonomi CA, Borgel SD, Carter JP, et al. Increased antitumor activity of bevacizumab in combination with hypoxia inducible factor-1 inhibition. Mol Cancer Ther 2009;8:1867-77.
44. Wang GL, Jiang BH, Rue EA, Semenza GL. Hypoxia-inducible factor 1 is a basic-helix-loop-helix-PAS heterodimer regulated by cellular O2 tension. Proc Natl Acad Sci U S A 1995;92:5510-4.
45. Huang T, Civelek AC, Li J, Jiang H, Ng CK, Postel GC, et al. Tumor microenvironment-dependent 18F-FDG, 18F-fluorothymidine, and 18F-misonidazole uptake: a pilot study in mouse models of human non-small cell lung cancer. J Nucl Med 2012;53:1262-8.
46. Huang T, Civelek AC, Zheng H, Ng CK, Duan X, Li J, et al. (18)F-misonidazole PET imaging of hypoxia in micrometastases and macroscopic xenografts of human non-small cell lung cancer: a correlation with autoradiography and histological findings. Am J Nucl Med Mol Imaging 2013;3:142-53.
47. Machulla H-J. Imaging of Hypoxia: Tracer Developments: Springer Science & Business Media; 2013.
48. Chen LQ, Pagel MD. Evaluating pH in the Extracellular Tumor Microenvironment Using CEST MRI and Other Imaging Methods. Adv Radiol 2015;2015.
49. Estrella V, Chen T, Lloyd M, Wojtkowiak J, Cornnell HH, Ibrahim-Hashim A, et al. Acidity generated by the tumor microenvironment drives local invasion. Cancer Res 2013;73:1524-35.
50. Gerweck LE. Tumor pH: implications for treatment and novel drug design. Semin Radiat Oncol 1998;8:176-82.
51. Gerweck LE, Seetharaman K. Cellular pH gradient in tumor versus normal tissue: potential exploitation for the treatment of cancer. Cancer Res 1996;56:1194-8.
52. Glunde K, Guggino SE, Solaiyappan M, Pathak AP, Ichikawa Y,

Bhujwalla ZM. Extracellular acidification alters lysosomal trafficking in human breast cancer cells. Neoplasia 2003;5:533-45.

53. Kato Y, Ozawa S, Miyamoto C, Maehata Y, Suzuki A, Maeda T, et al. Acidic extracellular microenvironment and cancer. Cancer Cell Int 2013;13:89.
54. Lindner D, Raghavan D. Intra-tumoural extra-cellular pH: a useful parameter of response to chemotherapy in syngeneic tumour lines. Br J Cancer 2009;100:1287-91.
55. Mahoney BP, Raghunand N, Baggett B, Gillies RJ. Tumor acidity, ion trapping and chemotherapeutics. I. Acid pH affects the distribution of chemotherapeutic agents in vitro. Biochem Pharmacol 2003;66:1207-18.
56. Raghunand N, Gillies RJ. pH and chemotherapy. Novartis Found Symp 2001;240:199-211; discussion 65-8.
57. Raghunand N, He X, van Sluis R, Mahoney B, Baggett B, Taylor CW, et al. Enhancement of chemotherapy by manipulation of tumour pH. Br J Cancer 1999;80:1005-11.
58. Webb BA, Chimenti M, Jacobson MP, Barber DL. Dysregulated pH: a perfect storm for cancer progression. Nat Rev Cancer 2011;11:671-7.

ABSTRACT(IN KOREAN)

이종이식 쥐 모델에서 항혈관형성 치료제제 투여 후 저산소증 PET방사선추적자 평가

<지도교수 윤미진>

연세대학교 대학원 의학과

조 아더 응혁

목적: 종양 저산소증은 고형암의 증식과 전이과정에 중요한 역할을 하는 것으로 알려져 있다. 일반적으로 종양 저산소증은 방사선치료와 항암요법 등과 같은 암 치료에 대해 높은 저항을 나타낼 뿐 아니라 종양의 악성도를 증가시키며 신생혈관 생성을 유도하고, 전이 발생을 증가시킨다고 알려져 있다. 그러므로 종양 저산소상태의 비침습적 확인은 종양의 악성도를 예측하고 치료계획을 세우기 위해 중요하며 암환자의 생존율 또한 저산소증에 지대한 영향을 받기 때문에 종양에서의 저산소증에 대한 연구와 영상을 이용한 탐지 방법은 근래 들어 광범위하게 연구되고 있다. ^{18}F-Fluoromisonidazole (^{18}F-MISO)와 ^{64}Cu-diacetyl-di(N_4-methylthiosemicarbazone) (^{64}Cu-ATSM)을 이용하여 양전자 방출 단층촬영(Positron Emission Tomography, PET)으로 저산소 상태를 평가할 수 있고 ^{18}F-fluorodeoxyglucose (^{18}F-FDG)은 세포의 당 대사 추적자로

종양의 저산소증과 관련되어 있는 것으로 알려져 있다. 이 연구의 목적은 이종이식 쥐에서 항혈관형성제제의 치료효과 평가하는데 있어서 ^{18}F-MISO, ^{64}Cu-ATSM, ^{18}F-FDG PET추적자들의 역할을 보고자 한다.

방법: 인간 대장암세포주인 HCT116을 1% O_2 저산소실이나 정상산소 배양실에 3시간과 15시간 배양한 후에 ^{18}F-FDG, ^{18}F-MISO, ^{64}Cu-ATSM을 넣고 방사선 섭취량을 측정하였다. 웨스턴블롯 분석 기법을 이용하여 HIF1a, GLUT-1의 발현 정도를 분석하였다. 추가적으로 세포외액의 환경에 따른 ^{18}F-MISO 섭취 영향을 평가하기 위하여 산성 세포배액에 같은 실험을 반복하였다. 그리고, 괴사한 세포에서 ^{18}F-MISO의 섭취 여부를 평가 하기 위하여 HCT116을 고열(55℃)를 유도하여 ^{18}F-MISO 섭취 실험하고, 장기간 저산소실에 보관하고 괴사를 유도한 후 같은 ^{18}F-MISO 실험을 반복하였다.

동물실험에서 항혈관형성제제인 Avastin의 치료 효과 평가하기 위하여 HCT116을 마우스 오른 뒷다리에 심었으며, 치료 전날 ^{18}F-FDG PET 끝난 후, 그 다음 날 ^{18}F-MISO이나 ^{64}Cu-ATSM PET을 치료 당일 날에 시행하였다. PET 촬영한 직후 Avastin 치료 시작하였으며 2주간 치료하였다. 치료 후 ^{18}F-FDG/^{18}F-MISO 나 ^{18}F-FDG/^{64}Cu-ATSM 조합으로 PET을 촬영하였다. PET촬영 직후 마우스를 희생하여, 종양을 적출하였다. 종양 조직의 반은 포르말린에 담궈 면역염색(pimonidazole, H&E, Ki-67) 진행하였고, 종양 조직의 남은 반은 cryosection하여 자가조직방사선촬영을 진행하였다.

결과: 세포실험에서 HCT116은 ^{18}F-MISO이나 ^{64}Cu-ATSM 방사선추적자들이 ^{18}F-FDG에 비해 저산소증환경에서 높은 섭취를

보였다. 웨스턴블롯 결과에서 HIF1a이 저산소증환경에서 안정화되었음을 확인하였으나 GLUT1 발현은 크게 일어나지 않았다. 산성환경 (pH 6.9)에서 ^{18}F-MISO 섭취가 50% 감소한 것을 확인하였고, ^{18}F-MISO이 괴사조건에서 정상산소환경보다 섭취 많은 것을 확인하였으나, 저산소환경 만큼 섭취되지 않았다.

동물연구에서 아바스틴 치료한 마우스에 심은 종양이 대조군에 비해 천천히 자랐으며, 면역염색결과에서 저산소 영역이 치료군에서 더 많았다 (17.67% ± 5.95 vs 11.02 ±4.81, p=0.004). 이에 반해 Ki67이나 괴사정도는 차이가 나지 않았다(36.02±24.8 vs27.82±14.0, p=0.249). 또한, 치료 후 PET에서 치료군이나 대조군에서 방사선 섭취량의 차이는 현저한 차이를 보이지 않았다 (^{18}F-FDG: 5.4±6.4, 3.0±1.8, p=0.123; ^{18}F-MISO: 4.6±3.0 vs 4.6±2.7, p=0.953). 자가조직방사선촬영 분석에서는 괴사된 부분에서 ^{18}F-MISO 섭취가(2.41±1.77) ^{18}F-FDG이나 (0.83±0.42, p=0.001) ^{64}Cu-ATSM 보다(0.94±0.48, p=0.005) 현저히 많았다.

결론: HCT116 대장암 피하조직 동물모델에서 아바스틴 치료 2주 후 종양증식억제가 관찰되었으며, 저산소범위가 증가되었다. 괴사 조직 평가 위하여 ^{64}Cu-ATSM가 ^{18}F-MISO보다 종양의 조직괴사 부분을 더 잘 반영하였다.

핵심되는 말 : 저산소증, ^{18}F-FDG, ^{18}F-MISO, ^{64}Cu-ATSM, 쥐 이종이식 암, 자가조직방사선촬영, 괴사